Different quantization behaviors of electrons confined in nanostructures at surfaces

S. Díaz-Tendero,[1,2] A. G. Borisov,[1,2] and J. P. Gauyacq[1,2]
[1]*Laboratoire des Collisions Atomiques et Moléculaires, CNRS, UMR 8625, Bâtiment 351, 91405 Orsay Cedex, France*
[2]*Laboratoire des Collisions Atomiques et Moléculaires, Université Paris-Sud, UMR 8625, Bâtiment 351, 91405 Orsay Cedex, France*
(Received 16 May 2007; revised manuscript received 16 August 2007; published 23 October 2007)

We show that two confinement modes exist for electronic states localized on a nanostructured surface. Image potential states confined on Ar islands on Cu(100) and on vacancy islands on 1 ML Ar/Cu(100) surface are studied. Whereas the Ar islands lead to the expected "particle-in-a-box" quantization, the vacancy islands are shown to exhibit a very different behavior, characterized by a much lower quantization energy. The two situations correspond to the confinement of two-dimensional surface-localized states on repulsive or attractive areas of the surface, and one should thus be as common as the other.

DOI: 10.1103/PhysRevB.76.155428 PACS number(s): 73.20.−r, 72.10.Fk, 73.21.−b, 77.55.+f

Atom manipulation brought the possibility of designing nanostructures at surfaces and of tailoring the electronic properties of the surface, opening the way toward fascinating physics and potential applications. The two-dimensional (2D) states localized at and propagating along the surface (e.g., the surface electronic states at the surface of noble metals) can be guided, trapped, or focused by artificial structures. The basic underlying quantum mechanical phenomena are the scattering and the confinement of the continuum electronic states. A continuum is associated with states delocalized over the entire space, restricting the system to a finite size brings confinement effects in, and a discrete set of quantized states appears inside the finite size object. The quantum corrals and quantum mirages represent spectacular examples of the effect of confinement of the surface-localized electronic states inside an artificial structure.[1–4] Besides these, surface science provides a whole series of examples of electron confinement in nanostructures as evidenced by scanning tunneling microscopy (STM), photoemission experiments, and theoretical studies. Electron confinement of 2D surface state, image potential states, and quantum well continua has been observed in adsorbate and adatom islands,[5–8] in vacancy islands,[9] and in terraces bounded by steps.[10–13] Electron confinement in one-dimensional structures such as segments of atomic wires has also been reported.[14,15]

A more or less general point of view has emerged from these detailed studies about the dynamics (energy and lifetime) of electronic states confined by a nanostructure. First, the translational invariance parallel to the surface is broken and scattering at the edge of the nanostructure opens new decay channels for the population of the confined states: an electron can be scattered into substrate bulk states or into the parent surface 2D continuum. Second, the energy of the confined states studied so far exhibits a "particle-in-a-box" kind of quantization, as if the nanostructure edges were replaced by infinite hard walls. A very nice example is provided by Ag(111) and Cu(111) surfaces with hexagonal adatom and vacancy islands of variable size. STM and theoretical results[5,9,16,17] showed that the 2D surface state continuum is quantized on the nanostructure. Island-localized states appear with energies corresponding to what is expected for a 2D electronic wave in an hexagon bounded by hard walls. These states are higher in energy than the bottom of the 2D surface state continuum on the infinite surface. The energy shift with respect to the bottom of the parent continuum, called the "quantization energy" below, scales proportionally to $1/R^2$, where R is the radius of the island.

We show in this paper that there are many cases where confinement of a 2D electronic continuum on a surface nanostructure does not lead to a particle-in-a-box behavior with quantization energy diverging when the nanostructure size goes to zero. In fact, there exist two classes of confining nanostructures at surfaces: one can be represented by a particle-in-a-box modeling, whereas the other does not and leads to much smaller quantization energies. We illustrate this effect by comparing the confinement of the image potential states on two different islands: (i) Ar islands on Cu(100) and (ii) clean Cu(100) patches in a 1 ML (monolayer) Ar/Cu(100) surface (called vacancy islands below). These two systems are schematically presented in Fig. 1. Confinement appears to be very different for the two types of islands, and we show how this is related to the attractive or repulsive character of the islands and to the 2D nature of the image state continua.

Image potential states (ISs) appear when an excited electron is trapped in front of the metal surface by the interaction with its self-induced polarization charge.[18,19] Far from the surface, this interaction converges to the classical image potential. When electron penetration into the metal is prohibited by the projected band gap, ISs are stationary within a one-electron picture and decay by inelastic electron-electron interactions inside the metal.[20] For surfaces such as Cu(100), where the surface-projected band gap overlaps the vacuum level, a whole Rydberg-like series of the ISs exists with energies given by $E_n=-1/32(n+a)^2+k_{\|}^2/2m^*$ (in a.u.). Here, E_n is the energy of the IS with respect to the vacuum level, n is the principal quantum number, $k_{\|}$ is the electron momentum parallel to the surface, m^* is the effective mass, and a is a

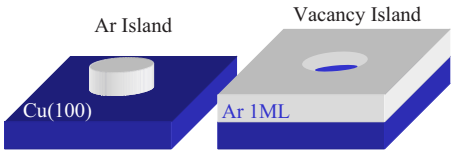

FIG. 1. (Color online) Schematic picture of the Ar islands and vacancy islands on a Cu(100) surface.

quantum defect. Due to their location at the metal-vacuum interface, ISs are strongly influenced by the surface condition. For example, the effect of a complete dielectric adsorbate layer on the surface is well documented both experimentally and theoretically.[21–23] If the energy of the IS is inside the dielectric band gap, its wave function is rejected further in vacuum leading to a decrease of the IS binding energy and of its decay rate [see, e.g., Ref. 23 for Ar/Cu(100)]. In the case of an incomplete Ar coverage of Cu(100) studied in the present work, confinement can occur on an Ar island surrounded by clean Cu(100) or on a clean Cu(100) island surrounded by a 1 ML thick Ar coverage (see Fig. 1). A recent theoretical study[24] showed that the energies of the ISs confined on Ar islands behave according to the "standard" particle-in-a-box model. However, we demonstrate here that, in the case of a vacancy island inside a 1 ML Ar coverage and situations alike, a very different physical picture has to be adopted.

The present theoretical study is based on a joint model potential and wave-packet propagation (WPP) approach where the dynamics of the IS electron in a model potential is studied in the time domain. A similar methodology has been used in our earlier studies of ISs on Cu(100) covered with Ar layers.[23,25] We consider islands (vacancy island in an Ar monolayer or Ar islands on a clean surface) with an approximately circular shape (see Fig. 1), i.e., all the Ar atoms within a given radius R from a central Ar atom are missing (included) in the vacancy (Ar island). The atomic positions are kept the same as in a full Ar monolayer. This approximation should not influence the main result of the present work about different quantization behaviors. Briefly, the interaction between an electron and the incomplete Ar layer is described by summing individual model electron-Ar interaction potentials, with all the mutual polarization and image interactions taken into account (see Ref. 25 for details). The electron-metal potential is adopted from Chulkov *et al.*[26] The latter is a model potential extracted from *ab initio* studies and adjusted to the Cu(100) electronic structure at $\bar{\Gamma}$. Free electron motion parallel to the surface is assumed. The electron-Ar nanostructure and the electron-metal interaction potentials are then summed to yield the total potential seen by an electron moving in front of the nanostructured surface. The time-dependent Schrödinger equation for the active electron in this potential is then solved by a three-dimensional WPP scheme, and all the information about the quasistationary states in the system is extracted: energies and decay rates (see Refs. 23, 24, and 27 for details). In this one-electron approach, the confined IS are quasistationary states that decay by electron transmission through the island edge.

Figure 2 presents the quantization energy for the lowest lying confined state deriving from the $n=1$ IS continuum on Ar islands and on vacancy islands. Results are presented as a function of $1/R^2$, where R is the island radius (the edge of the circular island is located at a distance $d/2$ from the outermost Ar, where d is the Ar-Ar distance). The quantization energy in the Ar island case[24] increases when the island radius decreases following a "particle-in-a-box" quantization which predicts a quantization energy proportional to $1/R^2$. In contrast, the quantization energy for a vacancy island saturates when the island radius decreases. This difference seems a striking result, since these two finite objects have exactly the same shape and they only differ by their edge: either a step up or down of a 1 ML thick Ar layer.

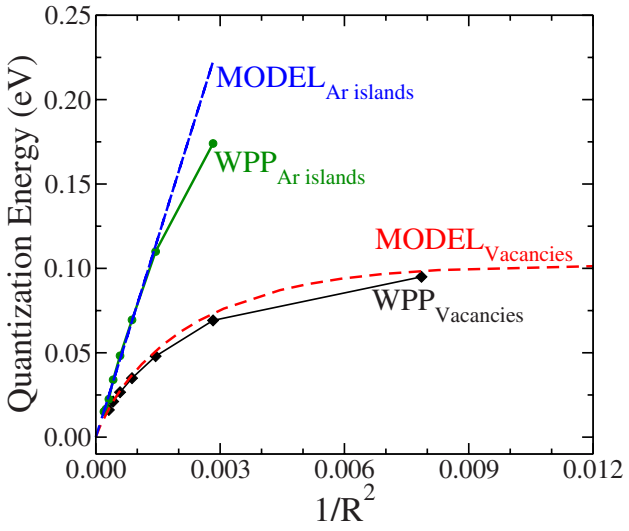

FIG. 2. (Color online) Quantization energy of the image potential states confined on Ar islands and on vacancy islands on Cu(100) as a function of $1/R^2$, where R is the island radius. The results obtained by 3D wave-packet propagation are represented by symbols joined by straight full lines: circles for the Ar islands and diamonds for the vacancy islands. The dashed lines represent the results of the 2D model (detailed in the text) for the Ar islands and vacancy islands.

Let us examine the differences between the two situations in more detail. In the case of a full Ar monolayer on Cu(100), the energy of the $n=1$ IS is higher than on the clean Cu(100) surface, because the image state wave function is repelled into vacuum where the image potential is weaker. At $\bar{\Gamma}$, this energy shift amounts to 0.102 eV (Ref. 23) for $n=1$. As a consequence, the $n=1$ IS confined on an Ar island can decay by electron scattering at the island edge into the $n=1$ IS continuum of the clean Cu surface. This decay channel is always open and it is very efficient.[24] Figure 3 presents the decay rate of the $n=1$ IS state confined on an Ar island as a function of $1/R^2$ (results taken from Ref. 24). In contrast, in the case of a vacancy island, the situation is reversed and the energy of the $n=1$ IS confined on a vacancy island is below the bottom of the $n=1$ IS on 1 ML Ar/Cu(100). Therefore, the only one-electron decay process is electron scattering at the island edge into the 3D propagating Cu bulk states. This process is much less efficient than the inter-IS scattering process, and the one-electron decay rates of ISs confined on vacancy islands are found to be at least 2 orders of magnitude smaller than those in the Ar island case (see Fig. 3). In both the Ar and the vacancy island cases, the one-electron decay rate of the confined IS is seen to decrease rapidly when the size of the islands increases, consistent with the fact that scattering at the island edges becomes less and less important when the size of the island increases. The decay rate shown in Fig. 3 only concerns one-electron transitions, while the confined IS can also decay by inelastic electron-

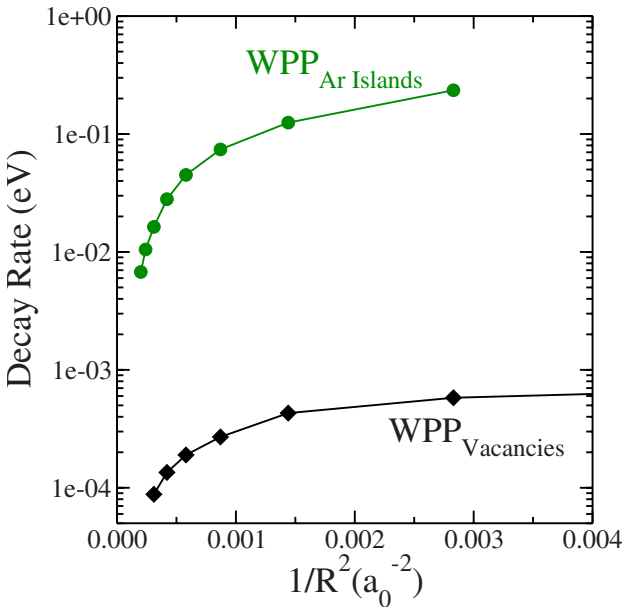

FIG. 3. (Color online) One-electron decay rate of the $n=1$ image potential states confined on Ar islands and on Ar vacancies on Cu(100). Green circles: Ar islands. Black diamonds: vacancy islands. The decay corresponds to the scattering of the image potential state at the edge of the confinement area. The decay rate (in eV) is presented as a function of $1/R^2$, where R is the radius of the confining structure.

electron interactions with the bulk electrons. The corresponding multielectron decay rate for the IS confined on a vacancy island should be close to the clean Cu(100) value around 16 meV.[20,28–30] In the vacancy island case, this multielectron rate is much larger that the one-electron decay rate and consequently, in that case, the confined ISs decay with a lifetime almost equal to that of the IS on a clean Cu(100) surface. This situation is thus quite different from the Ar island case, where for not very large islands, the confined ISs decay by scattering at the island edge (see discussion in Ref. 24).

The main difference between the Ar island and vacancy island systems comes from their attractive or repulsive character for an IS electron. In both cases, one can consider the system as an island surrounded by a homogeneous surface [either a clean Cu(100) or a 1 ML Ar/Cu(100) surface] and look at the island as a perturbation in the 2D IS continuum of the homogeneous surface. An Ar island appears as a repulsive area in the otherwise homogeneous surface, since on the island, the electron is repelled into a region where the image potential is weaker. In an opposite way, a vacancy island appears as an attractive area in the otherwise homogeneous surface, since in the vacancy, the electron can come closer to the metal where the image potential is stronger. Simon[31] has shown that in two dimensions, an attractive potential always bears a bound state. Even if the present system is not strictly speaking 2D (it is rather a 2D system imbedded in 3D), one can expect a vacancy island to always accommodate a bound state associated with the IS continuum, or more precisely, a quasistationary state decaying into the 3D bulk states. This is exactly what is observed in Fig. 2: the lowest lying confined

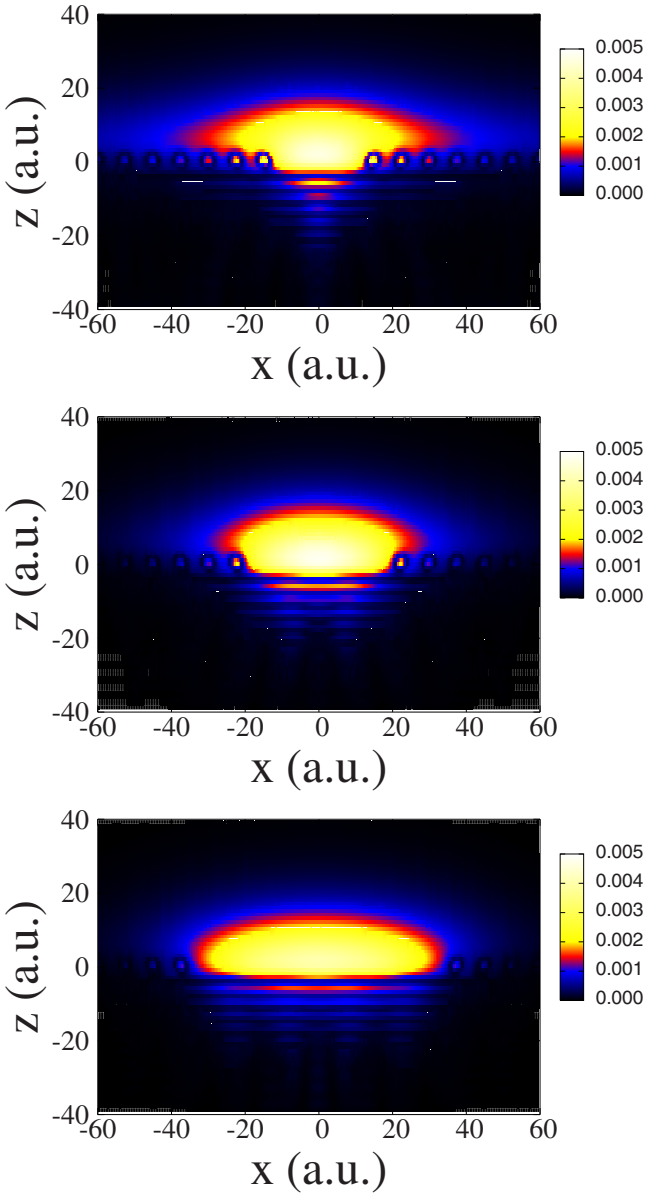

FIG. 4. (Color online) Contour plot of the electron density (arbitrary units) in the lowest lying confined state on a vacancy island. The density is shown in the (x,z) plane normal to the Cu surface that contains the center of the island. x is the coordinate parallel to the surface, and z is the coordinate perpendicular to the surface. The central missing atom of the vacancy is at the origin of the coordinates. Three different island diameters are presented: two, four, and eight times the Ar-Ar distance (from top to bottom). The color code is explained in the inset.

IS on the vacancy island always has a quantization energy lower than 0.102 eV, i.e., this state is always below the bottom of the IS continuum of 1 ML Ar/Cu(100). Thus, this 2D specific property accounts for the saturation of the quantization energy when the vacancy island size decreases. This phenomenon is analogous to the localization of the IS[32,33] and surface state continua by an attractive adsorbate.[34,35] In the present case, one can consider that the confined states on the vacancy islands correspond to the localization by the

attractive vacancy island of the 2D IS continuum on the full 1 ML Ar layer.

The above discussion also yields a qualitative recipe about where to look for the two different quantization regimes ("localization" or "particle-in-a-box"). Let us consider the case of a surface A and the case of the surface A with an overlayer B on it. *A priori*, IS on A and that on B/A are not at the same energy. If IS on A is lower in energy, then localization will occur on the vacancy islands, and if IS on B/A is lower, then it will occur on adsorbate islands. In both cases, the other situation will correspond to a "particle-in-a-box" quantization. One can also stress that in the localization case, scattering at the island edge should be weakly efficient, so that the confined levels would be narrow and long lived, at least as compared to the confined states in a "particle-in-a-box" regime. To our knowledge, cases where one would expect the localization type of quantization regime to appear have not been investigated experimentally up to now and only the "particle-in-a-box" quantization regime has been observed.

The above analysis can be further strengthened by considering a simple model of the IS localization on a vacancy island. We consider a 2D system with cylindrical symmetry to represent the IS electron moving parallel to the surface. The potential $V(\rho,\phi)$ is equal to $-V_0$ inside the vacancy island ($\rho \leqslant R$) and zero outside (ρ and ϕ are the cylindrical coordinates). V_0 is taken equal to the energy difference between the IS continuum on Cu(100) and on 1 ML Ar/Cu(100), i.e., 0.102 eV. The problem is invariant by rotation around the ϕ axis. The radial part of the wave function for $m=0$ symmetry (m is the projection of the angular momentum on the symmetry axis) is obtained as a regular J_0 Bessel function inside the island and a K_0 modified Bessel function outside. Matching J_0 and K_0 on the island boundary yields the quantization energy. The result for a continuous variation of the island radius is shown in Fig. 2 as the dashed line "$\text{MODEL}_{\text{Vacancies}}$." It is seen to accurately reproduce the full 3D WPP results. In particular, the saturation of the quantization energy is well reproduced in this 2D model. In contrast, quantization by a hard wall on the island boundary consists in imposing a zero of the J_0 Bessel function on the island boundary. This leads to a quantization energy proportional to $1/R^2$ that is shown as "$\text{MODEL}_{\text{Ar island}}$" in Fig. 2; it is seen to account for the quantization energy on the Ar island very well.

When the radius of the vacancy island decreases, the energy of the confined IS comes closer to the bottom of the IS continuum on 1 ML Ar/Cu(100) while remaining lower. This corresponds to a decrease of the binding energy of the confined IS with respect to the IS 2D continuum and thus to the lateral spreading of the confined state wave function. This point is illustrated in Fig. 4, which shows the electron density of the lowest lying confined IS state on vacancy islands of three different sizes (the diameter of the vacancy island corresponds to two, four, and eight Ar-Ar distances). The electron density is shown in the (z,x) plane, where z is the coordinate perpendicular to the surface and x is one of the coordinates parallel to the surface. The origin of coordinates is at the center of the vacancy. The IS electron appears to be nearly perfectly confined inside the largest vacancy island. In contrast, for the smallest vacancy island, the confined state significantly spreads outside the vacancy, in marked difference with a "particle-in-a-box model". One can also notice that for radii larger than the vacancy radius, the wave function does not penetrate into the Ar layer, and it is effectively repelled into vacuum as expected from the dielectric character of the layer. The wave functions in the Ar island case have been shown in Ref. 24; in that case, as expected for a "particle-in-a-box" quantization, the IS appears to be well localized on the islands for all radii.

In summary, we have shown how different finite size objects (Ar islands or vacancy islands) lead to different quantization behaviors of the image state on Cu(100). Due to the 2D nature of the image state continuum, quantization on a vacancy island on Ar/Cu(100) does not follow a "particle-in-a-box" behavior, and the quantization energy is seen to saturate as the island size decreases. This phenomenon can be seen as the localization of the 2D continuum by the vacancy island. This situation should be common on metal surfaces exhibiting a 2D continuum (surface state or image state). Indeed, in the case of an incomplete coverage by an adsorbate, one of the two objects, adsorbate islands or vacancy islands, should lead to this localization phenomenon, depending on the attractive or repulsive character of the adsorbate.

S.D.-T. gratefully acknowledges the Spanish Ministerio de Educación y Ciencia.

[1] M. F. Crommie, C. P. Lutz, and D. M. Eigler, Science **262**, 218 (1993).
[2] H. C. Manoharan, C. P. Lutz, and D. M. Eigler, Nature (London) **403**, 512 (2000).
[3] J. Kliewer, R. Berndt, and S. Crampin, Phys. Rev. Lett. **85**, 4936 (2000).
[4] K.-F. Braun and K.-H. Rieder, Phys. Rev. Lett. **88**, 096801 (2002).
[5] S. Pons, P. Mallet, and J.-Y. Veuillen, Phys. Rev. B **64**, 193408 (2001).
[6] L. Diekhöner, M. A. Schneider, A. N. Baranov, V. S. Stepanyuk, P. Bruno, and K. Kern, Phys. Rev. Lett. **90**, 236801 (2003).
[7] J. Li, W. D. Schneider, R. Berndt, and S. Crampin, Phys. Rev. Lett. **80**, 3332 (1998).
[8] F. Calleja, J. J. Hinarejos, A. L. Vázquez de Parga, and R. Miranda, Eur. Phys. J. B **40**, 415 (2004).
[9] L. Niebergall, G. Rodary, H. F. Ding, D. Sander, V. S. Stepanyuk, P. Bruno, and J. Kirschner, Phys. Rev. B **74**, 195436 (2006).
[10] Ph. Avouris and I.-W. Lyo, Science **264**, 942 (1994).
[11] J. E. Ortega, F. J. Himpsel, R. Haight, and D. R. Peale, Phys. Rev.

B **49**, 13859 (1994).
[12] L. Bürgi, O. Jeandupeux, A. Hirstein, H. Brune, and K. Kern, Phys. Rev. Lett. **81**, 5370 (1998).
[13] X. Y. Wang, X. J. Shen, R. M. Osgood, Jr., R. Haight, and F. J. Himpsel, Phys. Rev. B **53**, 15738 (1996).
[14] N. Nilius, T. M. Wallis, and W. Ho, Science **297**, 1853 (2002).
[15] S. Fölsch, P. Hyldgaard, R. Koch, and K. H. Ploog, Phys. Rev. Lett. **92**, 056803 (2004).
[16] J. Li, W.-D. Schneider, S. Crampin, and R. Berndt, Surf. Sci. **422**, 95 (1999).
[17] S. Crampin, M. H. Boon, and J. E. Inglesfield, Phys. Rev. Lett. **73**, 1015 (1994).
[18] P. M. Echenique and J. B. Pendry, J. Phys. C **11**, 2065 (1978).
[19] M. C. Desjonquères and D. Spanjaard, *Concepts in Surface Science*, Springer Series in Surface Science Vol. 40 (Springer-Verlag, Berlin, 1993).
[20] E. V. Chulkov, A. G. Borisov, J. P. Gauyacq, D. Sánchez-Portal, V. M. Silkin, V. P. Zhukov, and P. M. Echenique, Chem. Rev. (Washington, D.C.) **106**, 4160 (2006).
[21] D. F. Padowitz, W. R. Merry, R. E. Jordan, and C. B. Harris, Phys. Rev. Lett. **69**, 3583 (1992).
[22] M. Wolf, E. Knoesel, and T. Hertel, Phys. Rev. B **54**, R5295 (1996).
[23] D. C. Marinica, C. Ramseyer, A. G. Borisov, D. Teillet-Billy, J. P. Gauyacq, W. Berthold, P. Feulner, and U. Höfer, Phys. Rev. Lett. **89**, 046802 (2002).
[24] J. P. Gauyacq and A. G. Borisov, Surf. Sci. **600**, 825 (2006).
[25] D. C. Marinica, C. Ramseyer, A. G. Borisov, D. Teillet-Billy, and J. P. Gauyacq, Surf. Sci. **540**, 457 (2003).
[26] E. V. Chulkov, V. M. Silkin, and P. M. Echenique, Surf. Sci. **437**, 330 (1999).
[27] A. G. Borisov, A. K. Kazansky, and J. P. Gauyacq, Phys. Rev. B **59**, 10935 (1999).
[28] I. L. Shumay, U. Höfer, Ch. Reuß, U. Thomann, W. Wallauer, and Th. Fauster, Phys. Rev. B **58**, 13974 (1998).
[29] U. Höfer, I. L. Shumay, Ch. Reuß, U. Thomann, W. Wallauer, and Th. Fauster, Science **277**, 1480 (1997).
[30] I. Sarria, J. Osma, E. V. Chulkov, J. M. Pitarke, and P. M. Echenique, Phys. Rev. B **60**, 11795 (1999).
[31] B. Simon, Ann. Phys. (N.Y.) **97**, 279 (1976).
[32] A. G. Borisov, A. K. Kazansky, and J. P. Gauyacq, Phys. Rev. B **65**, 205414 (2002).
[33] J. P. Gauyacq, A. G. Borisov, and A. K. Kazansky, Appl. Phys. A: Mater. Sci. Process. **78**, 141 (2004).
[34] F. E. Olsson, M. Persson, A. G. Borisov, J. P. Gauyacq, J. Lagoute, and S. Fölsch, Phys. Rev. Lett. **93**, 206803 (2004).
[35] L. Limot, E. Pehlke, J. Kröger, and R. Berndt, Phys. Rev. Lett. **94**, 036805 (2005).